Catalysis Science & Technology

ROYAL SOCIETY OF CHEMISTRY

PAPER

View Article Online
View Journal

Open Access Article. Published on 29 December 2025. Downloaded on 1/23/2026 7:42:18 PM.
This article is licensed under a Creative Commons Attribution 3.0 Unported Licence.

Check for updates

Cite this: DOI: 10.1039/d5cy01306b

Ritter reactions in continuous flow catalysed by a solid-supported sulfonic acid catalyst

Lara J. Nolan,[abc] Ailbhe A. Ryan,[abc] Seán Dempsey,[abc] Megan Smyth,[c] Thomas S. Moody,[bc] Scott Wharry,[c] Karen Fahey,[b] Paul Dingwall,[a] David W. Rooney,[a] Jillian M. Thompson,*[a] Mark J. Muldoon*[a] and Peter C. Knipe*[a]

Received 31st October 2025,
Accepted 19th December 2025

DOI: 10.1039/d5cy01306b

rsc.li/catalysis

The Ritter reaction allows the 100% atom economical synthesis of amides *via* acid-catalysed coupling between nitriles and alcohol substrates. However, this reaction has traditionally required harsh acid catalysts which must be separated from the product stream. Here, we demonstrate that commercial polymer-supported Brønsted acids catalyse the Ritter reaction under continuous flow conditions. The products are generated in high yield and free from acidic catalyst impurities. Continuous flow conditions deliver high yields in significantly shorter reaction times compared with batch reactions (1 hour *vs.* 24 hours) and the catalyst remains effective after 43 hours of continuous operation.

Introduction

Amides are among the most important functional groups in all of chemistry (Fig. 1A). As well as occupying a central role in chemical biology within the structure of polypeptides, they are also present in many pharmaceutical compounds, with 16 of the 29 new small molecule drugs reported in 2021 containing at least one amide bond.[1] Amidations represent 25% of all reactions used in medicinal chemistry.[2] However, many established methods for amide bond formation (*e.g.* peptide couplings) require hazardous reagents or harsh conditions, alongside the generation of large quantities of chemical waste since they generally require stoichiometric activation of the acid.[3] Consequently, sustainable and scalable amide syntheses have been a long-standing research goal.

One approach towards amide synthesis is the Ritter reaction. The Ritter reaction is strategically distinct from typical amidations (where condensation of an amine with an activated carboxylic acid equivalent forms the central C–N bond), since the key bond-forming reaction generates the N–C_{alk} rather than the N–C═O bond.[4] It proceeds through initial acidic activation of an (typically secondary, tertiary or benzylic) alcohol or alkene, which is subsequently trapped by a nitrile (see Scheme 1). The resulting *N*-alkylnitrilium ion undergoes attack by water, with tautomerisation generating the desired amide product. The reaction was first reported by Ritter and Minieri in 1948, where alkenes and alcohols were activated with excess sulfuric acid to furnish amide products.[5] Catalytic variants have been developed to remove the need for stoichiometric loadings of harsh acids, which aim to maximize atom economy and minimize the *E*-factor[6] of such processes. Both Lewis and Brønsted acids are competent catalysts, as demonstrated in the literature over the past two decades.[7]

The first Ritter reaction deploying Brønsted acids in catalytic quantities was reported by Reddy at Bristol-Myers Squibb in 2003.[8] Sulfuric acid catalyst loadings of 47 mol% could be accessed when using an electron-rich nitrile, though

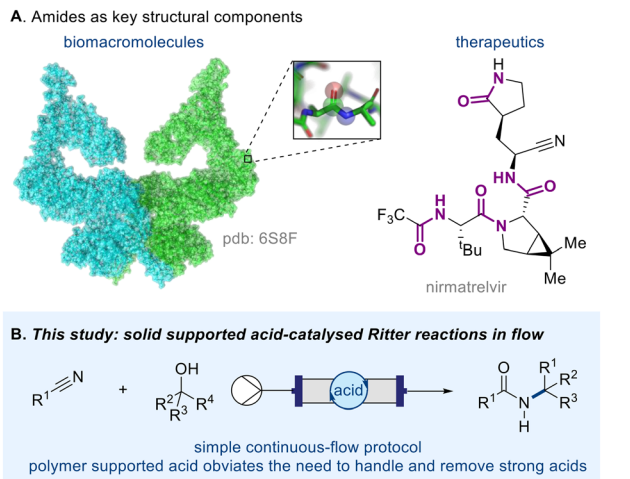

Fig. 1 Background and conception of this study: the importance of amides in medicinal chemistry and biochemistry, and concept of catalytic Ritter reactions under continuous flow conditions.

[a] School of Chemistry and Chemical Engineering, Queen's University Belfast, Belfast, BT9 5AG, UK. E-mail: p.knipe@qub.ac.uk; Web: https://www.knipechem.co.uk
[b] Arran Chemical Company, Athlone, Co., Roscommon, N37 DN24, Ireland
[c] Almac Group, Craigavon, BT63 5QD, UK

Open Access Article. Published on 29 December 2025. Downloaded on 1/23/2026 7:42:18 PM.
This article is licensed under a Creative Commons Attribution 3.0 Unported Licence.

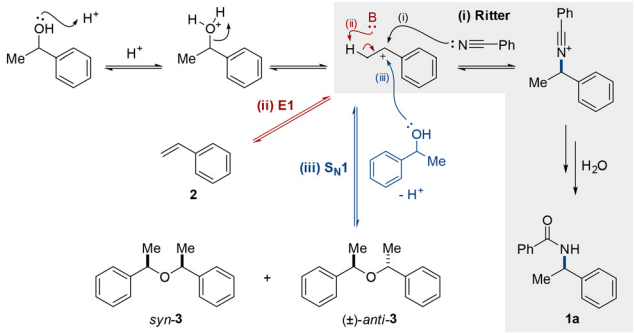

Scheme 1 Mechanism of the Ritter reaction (grey box) and for the formation of by-products: styrene **2** and ethers *syn*-**3** and (±)-*anti*-**3** *via* E1 (in red) and S_N1 (in blue) pathways respectively.

the reaction was only demonstrated for acetate substrates rather than unactivated alcohols. This approach was significantly improved by Sanz *et al.*, who showed that sulfonic acid catalysts could catalyse Ritter reactions at loadings as low as 5 mol%.[9]

The reaction has been deployed in numerous total syntheses and other synthetic chemistry applications.[4a,10] However, handling strong acids can be challenging since these are typically highly corrosive and toxic, and they must be separated from the products on completion of the reaction. Scale-up presents further challenges, with reports of violent exothermic runaway of reactions.[11] One solution to such safety concerns is to conduct reactions under continuous flow conditions,[12] where the acid catalyst can be quenched immediately after the reaction, reducing the amount of acid present to the flow reactor volume alone. In 2012 Wirth *et al.* reported the first Ritter reaction conducted in flow, reacting acetate substrates with nitriles in the presence of sulfuric acid.[13] Lewis acid catalysts have also been explored, with Nguyen *et al.* using tropylium tetrafluoroborate catalysts to promote Ritter reactions under continuous flow with loadings of just 1 mol%.[14] In all cases thus far reported, the reactions require a quench and subsequent separation of the acid catalyst from the reaction stream. There are few reports on the use of heterogeneous catalysts for Ritter-type transformations, but those that do use this approach report streamlined purification and catalyst recyclability.[15] During the studies described in this article, Yamada *et al.* reported Ritter reactions run under continuous flow using their previously disclosed *meta*-phenolsulfonic acid-formaldehyde (PAFR II) acidic resin.[16] The reaction displays good yields for several tertiary alcohol substrates, though the sole secondary alcohol substrate (cyclopentanol) gives a more modest yield of 23%. The reaction also requires the addition of 15 equivalents of acetic acid to proceed. In this context, this work aims to develop a robust continuous flow Ritter reaction which makes use of a commercial heterogenized acid catalyst to generate high value amide products from cheap and readily available starting materials, without the need for any additional acid solvents or co-catalysts (Fig. 1B).

Results and discussion

Batch catalyst screening

At the outset of our investigations, a series of experiments were conducted under batch operation to evaluate the key reaction parameters. Catalyst screening studies considered a range of solid-supported acidic resins for potential catalytic activity in the reaction of 1-phenylethanol with benzonitrile, as solvent, to generate amide **1a** (Fig. 2, see Table S1 for a comparison of the resins used). The formation of styrene **2** as a side-product (see Scheme 1) was also monitored. Literature precedent indicates that high reaction temperatures are a prerequisite, and hence studies were initially carried out at 100 °C.[15b,17] Good yields were achieved using Brønsted acid catalysts: Nafion™ NR50, polymer-supported *p*-toluene sulfonic acid (p-TSA$_R$), Amberlyst™ 15, and Amberlite™ HPR2900 (the latter two of which are styrene divinylbenzene polymers with sulfonic acid functional groups), though significant formation of styrene **2** was observed in all cases. p-TSA$_R$ displayed the fastest conversion to product, while Amberlyst™ 15, and Amberlite™ HPR2900H gave very similar reaction profiles, consistent with the structural similarities between them (see Table S1). Though also a polymer-supported arylsulfonic acid, the higher activity of the p-TSA$_R$ resin relative to these may be due to subtle differences in acid site accessibility or microenvironment. No product formation was observed on application of the Lewis acidic trityl chloride resin. Reaction temperature was found

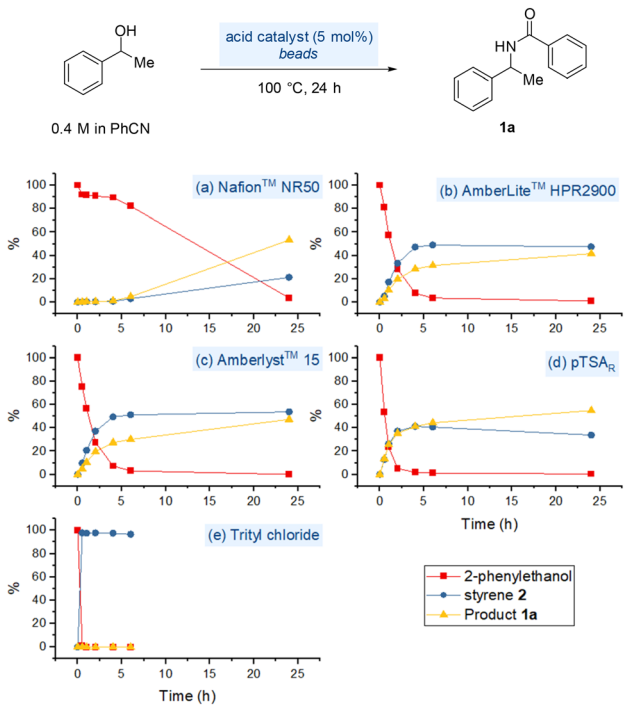

Fig. 2 Time course profiles of the acid catalyst screen conducted for the reaction between 1-phenylethanol and benzonitrile. Catalysts used in bead form. Individual data points were determined by GC/FID with a dodecane internal standard. For complete experimental data refer to the SI.

This journal is © The Royal Society of Chemistry 2026

Open Access Article. Published on 29 December 2025. Downloaded on 1/23/2026 7:42:18 PM.
This article is licensed under a Creative Commons Attribution 3.0 Unported Licence.

to have minimal effect on reaction efficacy in the range of 80–120 °C, except in the case of the Nafion™ NR50 resin where an increase in reaction rate was noted with increased reaction temperature post-induction period (see Fig. S1); this may be due to accelerated swelling of the Nafion™ NR50 at elevated temperatures. The presence of an induction period can be indicative of mass-transfer limitations at the outset of the reaction, or an autocatalytic mechanism. The fact that the induction period is eliminated when the catalyst is milled to a powder (see Fig. 3) supports the fact this is due to mass transfer limitations. This is consistent with the fact that – unlike Nafion™ NR50 – the other successful catalysts were all macroporous in structure (see Table S1). Though trityl chloride failed in forming the amide product, complete conversion of the starting material to styrene **2** was observed.

Product and styrene formation in the initial stages of reactions with arylsulfonic acid resins (Fig. 2b–d) is fast, but slows significantly once full conversion of the starting material is achieved. At this point, sluggish conversion of styrene to the product is also observed (see *e.g.* Fig. 2d and SI 2.2.3). The mechanism of the Ritter reaction is well-established as proceeding *via* a carbocationic intermediate, with both styrene **2** and bis(1-phenylethyl)ethers **3** plausible side-products *via* E1 and S_N1 pathways respectively (Scheme 1).[17d,18] To probe the formation of ethers **3**, the concentration of 1-phenylethanol was gradually increased in the presence of the three of the catalysts (Nafion™ NR50, Amberlyst™ 15, and *p*-TSA_R), and a correlation between increasing alcohol concentration and decreasing product yield was observed (see SI, section S2.2.3). Formation of the bis(1-phenylethyl)ether side-product **3** was unambiguously confirmed by its isolation. Suppression of its formation was achieved by conducting the reaction at a lower alcohol concentration of 0.2 m.

Significant quantities of styrene **2** were observed through a competing side-reaction, and attempts to suppress its formation were unsuccessful. However, we hypothesised that under the reaction conditions both **2** and **3** would be formed reversibly and could re-form the carbocation required for the formation of the Ritter product **1a**. This was demonstrated for **2** (see Fig. S3), and has previously been reported for **3**.[17d]

The catalysts used in these studies were relatively large beads of low surface area (see Table S1). To maximize exposure of the catalyst surface area, and hence minimize mass-transfer limitations, the three best performing catalysts were pulverized under milling conditions (see SI section S2.1.2) and re-examined. Pleasingly, near quantitative yields were observed in all cases when employing acid catalysts in their powdered form (Fig. 3). The more acidic fluorosulfonic acid-based Nafion™ NR50 gave the most rapid conversion, while *p*-TSA_R and AmberLyst™ 15 – both macroporous polymer-supported sulfonic acids, displayed similar conversion profiles. The surprising underperformance of Nafion™ NR50 at 20 mol% may be a consequence of batch variations in the pulverised catalyst, since its beads were much harder than the other resins.

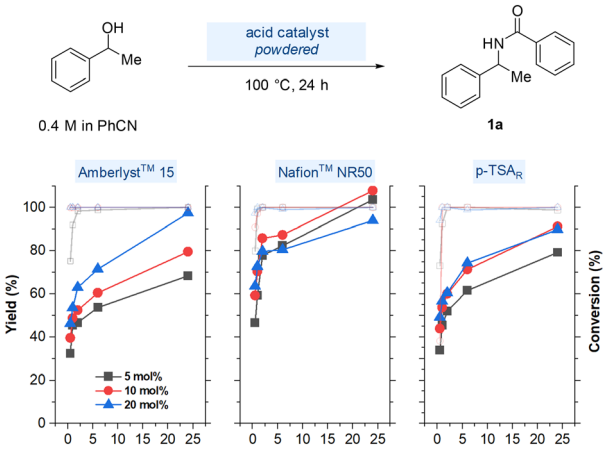

Fig. 3 Comparison of powdered catalyst activity at various loadings. Yields and conversions determined by GC/FID with a dodecane standard. Dark lines and filled datapoints indicate product yields; pale lines and open datapoints indicate conversion. For complete experimental data refer to the SI.

Continuous flow studies

The transfer of this process from batch to continuous flow operation was then undertaken. The flow reactor design used featured a single peristaltic pump, stainless steel fixed bed reactor (FBR), and 5 bar back pressure regulator (BPR) to regulate flow. Connections between the flow path were made using PTFE tubing (0.75 mm internal diameter) and PEEK/PFE nuts/ferrules. Operationally, a solution of the appropriate alcohol dissolved in the nitrile coupling partner was delivered to the FBR which contained the solid supported acid catalyst in bead form. The FBR was housed in an oven to ensure an even heat distribution throughout the reactor (Scheme 2).

High-temperature continuous-flow use of immobilised Brønsted acids is well-precedented. Amberlyst™ 36 sulfonic acid resins have been operated in pressurised packed-bed and biphasic fixed-bed reactors at 130 °C for continuous carbohydrate dehydration extraction chemistry,[19] while silica-supported sulfonic acids were used at temperature of up to 180 °C for the silyl protection of alcohols[20] and 110 °C for Fischer esterification.[21] For all continuous flow studies polymer supported acids were used as supplied in their bead form, since we felt this would be more reproducible and ease implementation by other researchers. Due to its high price, procurement challenges, and increasing regulatory restrictions on the use of PFAS,[22] we elected not to take Nafion™ NR50 forward. As such, only Amberlyst™ 15 and

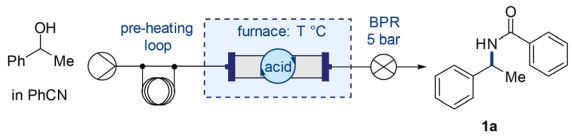

Scheme 2 Design for a flow reactor enabling continuous operation of the Ritter reaction with solid-supported sulfonic acid catalysts.

Open Access Article. Published on 29 December 2025. Downloaded on 1/23/2026 7:42:18 PM.
This article is licensed under a Creative Commons Attribution 3.0 Unported Licence.

p-TSA$_R$ were considered for application under a continuous flow regime (Fig. 4).

For both catalysts increasing the residence time led to a greater yield of the desired amide (Fig. 4A). At short residence times, large amounts of the styrene by-product **2** were observed. However, upon increasing the residence time, the yield of this by-product was significantly reduced, with a concomitant increase in the product yield. This is consistent with the reversible mechanism indicated in Scheme 1, and indicates that the styrene is the kinetic product of the reaction whilst the amide **1a** is the thermodynamic product. Of the catalyst/residence time pairs considered, maximum yields of the amide product were obtained when using a *p*-TSA$_R$ catalyst and residence time of 30 min. Increasing reaction temperature from 80 to 120 °C resulted in a gradual increase in product yield, but a further increase in temperature to 150 °C led to a decreased yield of the desired product, increased styrene formation, and overall reduced mass balance relative to 120 °C (Fig. 4B). While the thermal stability of *p*-TSA$_R$ is not reported, this may be a result of decomposition of the acid catalyst.

Further increasing the residence time to 1 h by doubling the amount of acidic resin ultimately allowed the desired amide to be obtained in 90% yield at 120 °C at an alcohol concentration of 0.2 M (Fig. 4C). Increasing the alcohol concentration further did not promote a shift in selectivity in favour of the styrene by-product **2**. Though product conversion was complete in all cases, overall product yields were reduced at higher concentrations (from 90% at 0.2 M to 76% at 0.8 M). This is likely due to increased formation of the ether by-product **3**, as observed at high alcohol concentrations during batch studies. A concentration of 0.2 M was therefore used in subsequent studies. Using our optimised conditions for continuous flow operation, we sought to explore the scope of our protocol in terms of both functional group compatibility and structural diversity of the substrates (Scheme 3). Reactions with 1-phenylethanol demonstrated that several nitriles are tolerated, with

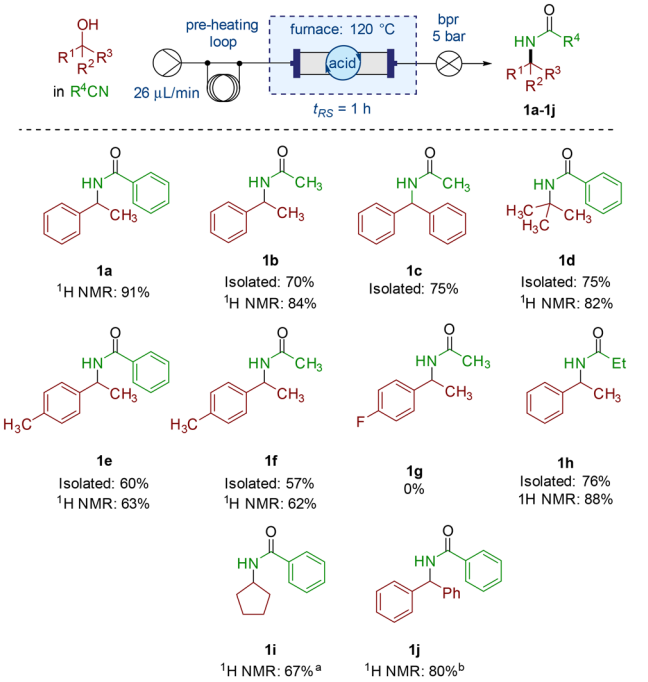

Scheme 3 Exploration of substrate scope of Ritter reaction under continuous flow. Conditions: *p*-TSA$_R$ acid catalyst (1.14 g), alcohol (0.2 M in nitrile), residence time (1 h), temperature (120 °C). ^{1}H NMR yields were determined using internal standard mesitylene. [a]Conducted at an alcohol concentration of 0.1 M. [b]Use of ethyl acetate as a co-solvent in a ratio of 2 : 1, benzonitrile: ethyl acetate. For complete experimental data refer to the SI.

benzonitrile, acetonitrile and propionitrile all affording products in >70% isolated yield (**1a**, **1b**, **1h**). The reaction was further probed with several substituted 1-arylethanol substrates: a *para*-tolyl substrate reacted efficiently with both benzonitrile and acetonitrile under the reaction conditions (**1e**, **1f**) albeit in slightly reduced yield relative to the unsubstituted parent substrate. However, *para*-fluorophenyl product **1g** was not formed at all, with the reaction yielding only unreacted starting material. This

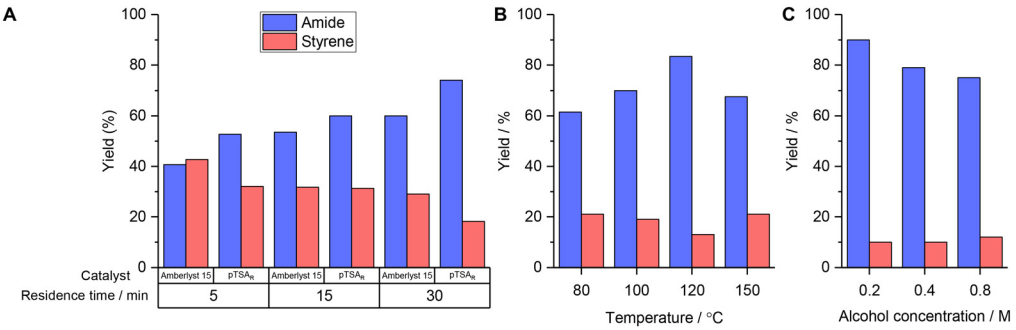

Fig. 4 Continuous flow parameter optimizations. Conversion was 100% in all cases except the 5 minute residence time Amberlyst™ 15 experiment, which reached 95% conversion. (A) Residence time screen conducted for *p*-TSA$_R$ and Amberlyst™ 15 catalysts (1-phenylethanol 0.2 M in PhCN, flow rate: 156, 52 and 26 µL min^{-1} for 5, 15 and 30 min residence times respectively, 100 °C). (B) Temperature screen (1-phenylethanol 0.2 M in PhCN, *p*-TSA$_R$ catalyst, flow rate: 26 µL min^{-1}, 30 min residence time), (C) concentration screen (1-phenylethanol in PhCN, *p*-TSA$_R$ catalyst, flow rate: 26 µL min^{-1}, 1 h residence time, 120 °C). Yields of the desired amide **1a** and styrene by-product **2** are indicated in blue and red respectively. Yields determined by GC/FID with a dodecane standard. For complete experimental data refer to the SI.

Open Access Article. Published on 29 December 2025. Downloaded on 1/23/2026 7:42:18 PM.
This article is licensed under a Creative Commons Attribution 3.0 Unported Licence.

is likely due to the electron-withdrawing nature of the fluoro group destabilizing the benzylic cation required for the reaction to proceed (see Scheme 1). With no ability to form competing elimination by-products such as **2**, and a high capacity to stabilize the carbocationic intermediate, diphenylmethanol was expected to perform well as a substrate. When reacting diphenylmethanol with benzonitrile, although NMR indicated quantitative yields had been achieved, a significant amount of precipitation (assumed to be the amide product **1j**) accumulated and resulted in reactor fouling. Attempts to overcome this *via* altering the reactor design and alcohol concentration failed (Fig. S6). The addition of ethyl acetate to the reaction as a co-solvent in a 2 : 1 ratio of benzonitrile : ethyl acetate afforded the desired amide in 80% yield; while this yield is lower than that obtained in pure benzonitrile, this approach allowed operation under continuous flow without reactor fouling. The reaction of diphenylmethanol with acetonitrile suffered no such fouling issues, and proceeded under the optimized conditions to form the product **1c** in 75% yield. Lastly, it was demonstrated that the procedure was amenable to tertiary and secondary aliphatic alcohols lacking benzylic stabilization, with *N-tert*-butyl and cyclopentyl amides **1d** and **1i** formed in 75% and 67% isolated yields respectively. The demonstrated scope complements well the work of Yamada *et al.*,[16] where substrates were largely formed from tertiary alcohols. Under our conditions, **1i** is formed in 67% yield under continuous flow, a significant improvement of the 23% yield attained in that study.

We lastly sought to determine whether the catalytic system could be run continuously for a prolonged period, or whether this would be prevented by catalyst degradation. Using p-TSA$_R$ as the catalyst, the reaction of 1-phenylethanol and benzonitrile at 100 °C was studied under continuous operation over 43 h.[23] An initial spike in product yield to 90% was observed, followed by a drop to a lower steady-state output (Fig. 5). After approximately 3 reactor volumes had been processed steady-state was achieved. No physical change in the catalyst was observed, and the initial spike may reflect transient start-up behaviour of the fresh acid resin, with the catalyst bed conditioning and equilibrating under flow to a lower steady-state activity. Over the course of the 43 h reaction the product yield decreased from 81% to 67%, indicating that the catalyst has significant resistance to degradation even over long periods at elevated temperature. Under steady-state operation (average yield 74%), the process operated with a space–time yield of approximately 33 g L^{-1} h^{-1}, demonstrating sustained reactor productivity over extended continuous operation.

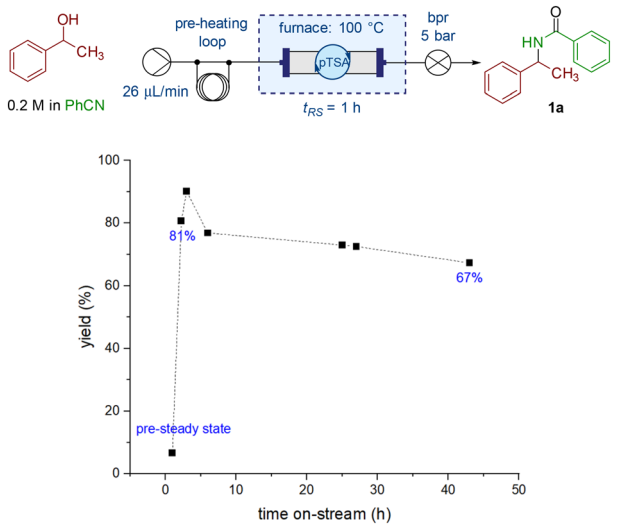

Fig. 5 Catalyst longevity study for the synthesis of **1a** under continuous flow conditions. Yields determined by GC/FID with a dodecane standard. For complete experimental data refer to the SI.

Conclusions

The successful development of the Ritter reaction under continuous flow operation in the presence of a heterogenized acid catalyst has been reported. Initial studies under batch operation guided the transfer of this process to flow. A range of commercially available polymer-supported acid resins were investigated with promising results in most cases. The effects of reaction temperature, concentration, and residence time were also evaluated, which led to suitable conditions for application to a continuous flow process which could be run for a prolonged time with minimal catalyst deactivation. Continuous flow avoided the formation of homo-coupled ether by-products observed during batch studies. The use of a solid acid catalyst also enabled the use of a simple reactor design, offered the potential for catalyst recycling, and afforded streamlined product purification by removing the need for tedious workup procedures. A range of amide products were obtained using this method, which showed a high tolerance for aromatic, aliphatic alcohol and nitrile substrates. Together, the robustness, versatility, and potential for immediate scale-up makes this technology an attractive route in the synthesis of amide products for both academic and industrial purposes.

Author contributions

LJN: investigation, visualization, writing – original draft, writing – review & editing; AAR: writing – review & editing; SD: writing – review & editing; MS: project administration, supervision, writing – review & editing; TSM: funding acquisition, resources, supervision, writing – review & editing; SW: supervision, writing – review & editing; KF: project administration, supervision, writing – review & editing; PD: writing – review & editing; DWR: funding acquisition, writing – review & editing; JMT: funding acquisition, supervision, writing – review & editing; MJM: conceptualization, funding acquisition, project administration, supervision, writing – review & editing; PCK: conceptualization, funding

Open Access Article. Published on 29 December 2025. Downloaded on 1/23/2026 7:42:18 PM.
This article is licensed under a Creative Commons Attribution 3.0 Unported Licence.

acquisition, project administration, supervision, writing – original draft, writing – review & editing.

Conflicts of interest

There are no conflicts to declare.

Data availability

The data supporting this article have been included as part of the supplementary information (SI).

Supplementary information: experimental procedures, characterisation data, supplementary figures and discussion. See DOI: https://doi.org/10.1039/d5cy01306b.

Acknowledgements

This project received funding from the European Union's Horizon 2020 Research and Innovation Programme under Marie Skłodowska-Curie Grant Agreement 813394. This publication contains the views of the authors, and the European Commission is not responsible for any use that may be made of the information it contains.

Notes and references

1 S. Yuan, D.-S. Wang, H. Liu, S.-N. Zhang, W.-G. Yang, M. Lv, Y.-X. Zhou, S.-Y. Zhang, J. Song and H.-M. Liu, *Eur. J. Med. Chem.*, 2023, **245**, 114898.
2 (*a*) J. Boström, D. G. Brown, R. J. Young and G. M. Keserü, *Nat. Rev. Drug Discovery*, 2018, **17**, 709; (*b*) D. G. Brown and J. Boström, *J. Med. Chem.*, 2016, **59**, 4443.
3 J. Magano, *Org. Process Res. Dev.*, 2022, **26**, 1562.
4 (*a*) M.-E. Chen, X.-W. Chen, Y.-H. Hu, R. Ye, J.-W. Lv, B. Li and F.-M. Zhang, *Org. Chem. Front.*, 2021, **8**, 4623; (*b*) G. Mohammadi Ziarani, F. Soltani Hasankiadeh and F. Mohajer, *ChemistrySelect*, 2020, **5**, 14349.
5 (*a*) J. J. Ritter and J. Kalish, *J. Am. Chem. Soc.*, 1948, **70**, 4048; (*b*) J. J. Ritter and P. P. Minieri, *J. Am. Chem. Soc.*, 1948, **70**, 4045.
6 R. A. Sheldon, *Green Chem.*, 2017, **19**, 18.
7 A. Guérinot, S. Reymond and J. Cossy, *Eur. J. Org. Chem.*, 2011, **2012**, 19.
8 K. L. Reddy, *Tetrahedron Lett.*, 2003, **44**, 1453.
9 R. Sanz, A. Martínez, V. Guilarte, J. M. Álvarez-Gutiérrez and F. Rodríguez, *Eur. J. Org. Chem.*, 2007, **2007**, 4642.
10 (*a*) M. Biermann, G. Zheng, M. Hojahmat, N. V. Moskalev and P. A. Crooks, *Tetrahedron Lett.*, 2015, **56**, 2608; (*b*) M. Henrot, A. Jean, P. A. Peixoto, J. Maddaluno and M. De Paolis, *J. Org. Chem.*, 2016, **81**, 5190; (*c*) B. V. Subba Reddy, S. Ghanty, N. S. S. Reddy, Y. J. Reddy and J. S. Yadav, *Synth. Commun.*, 2014, **44**, 1658; (*d*) D. B. Vu, T. V. Nguyen, S. T. Le and C. D. Phan, *Org. Process Res. Dev.*, 2017, **21**, 1758.
11 (*a*) S.-J. Chang, *Org. Process Res. Dev.*, 1999, **3**, 232; (*b*) W. O. Fugate and M. J. D'Errico, *USA Pat.*, 3151157, 1964; (*c*) S. Veedhi and S. R. Babu, *Org. Process Res. Dev.*, 2013, **17**, 1597.
12 A. I. Alfano, H. Lange and M. Brindisi, *ChemSusChem*, 2022, **15**, e202102708.
13 L. Audiger, K. Watts, S. C. Elmore, R. I. Robinson and T. Wirth, *ChemSusChem*, 2012, **5**, 257.
14 S. H. Doan, M. A. Hussein and T. V. Nguyen, *Chem. Commun.*, 2021, **57**, 8901.
15 (*a*) L. M. M. Mesquita, R. M. A. Pinto, J. A. R. Salvador, J. H. Clark and V. L. Budarin, *Catal. Commun.*, 2015, **69**, 170; (*b*) M. Mokhtary and G. Goodarzi, *Chin. Chem. Lett.*, 2012, **23**, 293; (*c*) T. Okuhara and X. Chen, *Microporous Mesoporous Mater.*, 2001, **48**, 293; (*d*) V. Polshettiwar and R. S. Varma, *Tetrahedron Lett.*, 2008, **49**, 2661; (*e*) R. K. Rapolu, B. Nabamukul, S. R. Bommineni, R. Potham, N. Mulakayala and S. Oruganti, *RSC Adv.*, 2013, **3**, 5332; (*f*) F. Tamaddon, M. Khoobi and E. Keshavarz, *Tetrahedron Lett.*, 2007, **48**, 3643.
16 E. Soliman, H. Baek, N. Mase and Y. M. A. Yamada, *J. Org. Chem.*, 2025, **90**, 1447.
17 (*a*) N. Ajvazi and S. Stavber, *Catalysts*, 2020, **10**, 460; (*b*) L. R. Jefferies and S. P. Cook, *Tetrahedron*, 2014, **70**, 4204; (*c*) T. Tang, L. Zhang, H. Dong, Z. Fang, W. Fu, Q. Yu and T. Tang, *RSC Adv.*, 2017, **7**, 7711; (*d*) M. Ueno, R. Kusaka, S. D. Ohmura and N. Miyoshi, *Eur. J. Org. Chem.*, 2019, **2019**, 1796.
18 L. I. Krimen and D. J. Cota, *Org. React.*, 1969, **17**, 213.
19 (*a*) S. Souzanchi, L. Nazari, K. T. V. Rao, Z. Yuan, Z. Tan and C. C. Xu, *New J. Chem.*, 2021, **45**, 8479; (*b*) C. Aellig, D. Scholz, P. Y. Dapsens, C. Mondelli and J. Pérez-Ramírez, *Catal. Sci. Technol.*, 2015, **5**, 142.
20 S. A. Van Den Berg, R. A. M. Frijns, T. Wennekes and H. Zuilhof, *J. Flow Chem.*, 2015, **5**, 95.
21 A. Furuta, T. Fukuyama and I. Ryu, *Bull. Chem. Soc. Jpn.*, 2017, **90**, 607.
22 ECHA Hot Topics: Per- and polyfluoroalkyl substances (PFAS), https://echa.europa.eu/hot-topics/perfluoroalkyl-chemicals-pfas, (accessed 30th October 2025).
23 *p*-TSA was utilized for the initial longevity study as it was noted that Amberlyst 15 demonstrates degradation at high temperatures.

 This journal is © The Royal Society of Chemistry 2026